CHAPTER 10. STRATOSPHERIC OZONE

The stratospheric ozone layer, centered at about 20 km above the surface of the Earth (Figure 10-1), protects life on Earth by absorbing UV radiation from the Sun. In this chapter we examine the mechanisms controlling the abundance of ozone in the stratosphere and the effect of human influence.

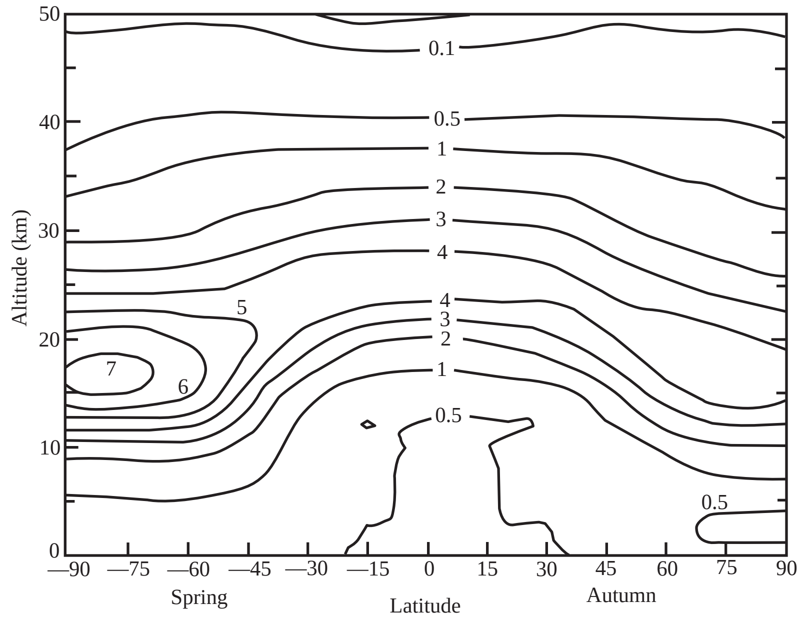

Figure 10-1 The natural ozone layer: vertical and latitudinal distribution of the ozone number density (10^{12} molecules cm^{-3}) at the equinox, based on measurements taken in the 1960s. From Wayne, R.P., *Chemistry of Atmospheres,* Oxford, 1991.

10.1 CHAPMAN MECHANISM

The presence of a high-altitude ozone layer in the atmosphere was first determined in the 1920s from observations of the solar UV spectrum. A theory for the origin of this ozone layer was proposed in 1930 by a British scientist, Sydney Chapman, and is known as the *Chapman mechanism.* It lays the foundation for current understanding of stratospheric ozone.

10.1.1 The mechanism

Chapman proposed that the ozone layer originates from the photolysis of atmospheric O_2. The bond energy of the O_2 molecule (498 kJ mol^{-1}) corresponds to the energy of a 240 nm UV photon;

only photons of wavelengths less than 240 nm can photolyze the O_2 molecule. Such high-energy photons are present in the solar spectrum at high altitude (Figure 10-2). Photolysis of O_2 yields two O atoms:

$$O_2 + h\nu \rightarrow O + O \qquad (\lambda < 240 \text{ nm}) \tag{R1}$$

where the O atoms are in the ground-level triplet state $O(^3P)$ (section 9.4) and are highly reactive due to their two unpaired electrons. They combine rapidly with O_2 to form ozone:

$$O + O_2 + M \rightarrow O_3 + M \tag{R2}$$

where M is a third body (section 9.1.2).

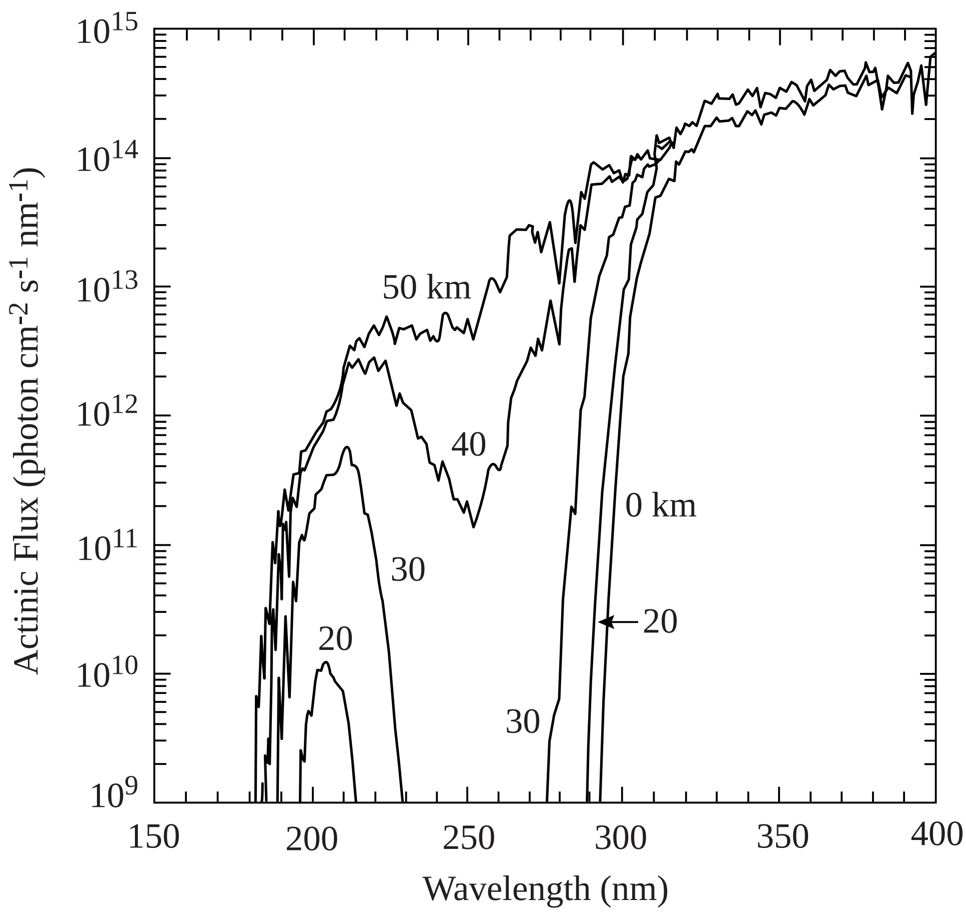

Figure 10-2 Solar actinic flux at different altitudes, for typical atmospheric conditions and a 30^o solar zenith angle. From DeMore, W.B., et al., *Chemical Kinetics and Photochemical Data for Use in Stratospheric Modeling,* JPL Publication 97-4, Jet Propulsion Lab, Pasadena, CA, 1997.

The O_3 molecules produced in reaction *(R2)* go on to photolyze. Because the bonds in the O_3 molecule are weaker than those in the O_2 molecule, photolysis is achieved with lower-energy photons:

$$O_3 + h\nu \rightarrow O_2 + O(^1D) \qquad (\lambda < 320\ \text{nm})$$
$$O(^1D) + M \rightarrow O + M$$

$$\text{Net:}\quad O_3 + h\nu \rightarrow O_2 + O \qquad \text{(R3)}$$

where $O(^1D)$ is the O atom in an excited singlet state (section 9.4) and is rapidly stabilized to $O(^3P)$ by collision with N_2 or O_2. Note that *(R3)* is not a terminal sink for O_3 since the O atom product may recombine with O_2 by *(R2)* to regenerate O_3. For O_3 to actually be lost the O atom must undergo another reaction, which in the Chapman mechanism is

$$O_3 + O \rightarrow 2O_2 \qquad \text{(R4)}$$

10.1.2 Steady-state solution

A schematic for the Chapman mechanism is shown in Figure 10-3. Rate constants for reactions *(R1)-(R4)* have been measured in the laboratory. Reactions *(R2)* and *(R3)* are found to be much faster than reactions *(R1)* and *(R4)*, as might be expected from our discussion above. We thus have a rapid cycle between O and O_3 by reactions *(R2)* and *(R3)*, and a slower cycle between O_2 and $(O+O_3)$ by *(R1)* and *(R4)*. Because of the rapid cycling between O and O_3 it is convenient to refer to the sum of the two as a *chemical family*, odd oxygen ($O_x \equiv O_3 + O$), which is produced by *(R1)* and consumed by *(R4)*.

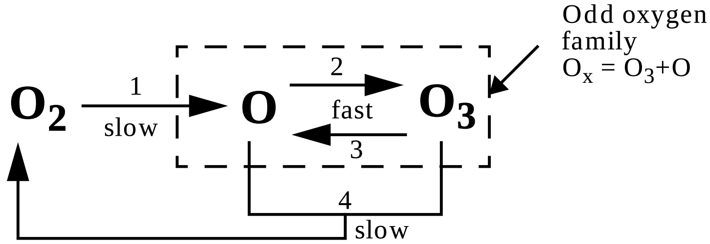

Figure 10-3 The Chapman mechanism

Simple relationships between O_2, O, and O_3 concentrations can be derived from a chemical steady-state analysis of the Chapman mechanism. As we saw in section 3.1.2, chemical steady state can be assumed for a species if its production and loss rates remain roughly constant over its lifetime. We first examine if chemical steady state is applicable to the shortest-lived species in Figure 10-3, the O atom. The lifetime τ_O of the O atom against conversion to O_3 by *(R2)* is

$$\tau_O = \frac{[O]}{k_2[O][O_2][M]} = \frac{1}{k_2[O_2][M]} \tag{10.1}$$

where we have used the low-pressure limit in the rate expression for *(R2)*, as is appropriate for atmospheric conditions. In equation *(10.1)*, [M] is the air number density n_a, and $[O_2] = C_{O2}n_a$ where C_{O2} = 0.21 mol/mol is the mixing ratio of O_2. Thus:

$$\tau_O = \frac{1}{k_2 C_{O2} n_a^2} \tag{10.2}$$

All terms on the right-hand side of *(10.2)* are known. Substituting numerical values one finds that τ_O in the stratosphere is of the order of seconds or less (problem 10. 2). Production and loss rates of the O atom depend on the meteorological environment (pressure, temperature, radiation) and on the O_3 abundance, neither of which vary significantly over a time scale of seconds. We can therefore assume chemical steady state for O atoms between production by *(R3)* and loss by *(R2)*, neglecting reactions *(R1)* and *(R4)* which are much slower:

$$k_2[O][O_2][M] = k_3[O_3] \tag{10.3}$$

Rearrangement of *(10.3)* yields

$$\frac{[O]}{[O_3]} = \frac{k_3}{k_2 C_{O2} n_a^2} \tag{10.4}$$

Substituting numerical values one finds $[O]/[O_3] << 1$ throughout the stratosphere (problem 10. 2). Observed concentrations (Figure

10-4) obey closely this steady state.

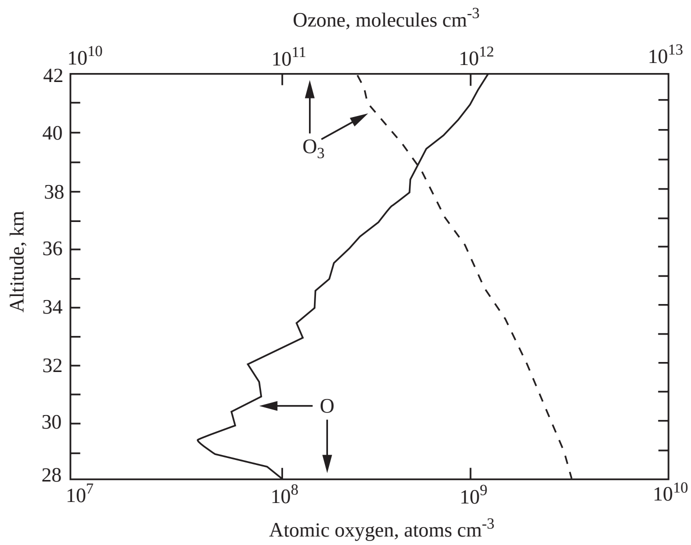

Figure 10-4 Simultaneous measurements of O and O_3 concentrations in the stratosphere over Texas in December 1977. Adapted from R.P. Wayne, *op. cit.*

An important result of our steady-state analysis for the O atom is that O_3 is the main component of the O_x family: $[O_x] = [O_3\} + [O] \approx [O_3]$. This result has two implications:

- The concentration of O_3 is controlled by the slow production and loss of O_x from reactions *(R1)* and *(R4)* rather than by the fast production and loss of O_3 from reactions *(R2)* and *(R3)*;
- The effective lifetime of O_3 against chemical loss is defined by the lifetime of O_x.

The lifetime of O_x is given by:

$$\tau_{Ox} = \frac{[O_x]}{2k_4[O][O_3]} \approx \frac{1}{2k_4[O]} \tag{10.5}$$

where we have included a factor of 2 in the denominator because *(R4)* consumes two O_x (one O_3 and one O). The factor of 2 can be derived formally from a mass balance equation for O_x as the sum of the mass balance equations for O_3 and O:

$$\begin{aligned} \frac{d}{dt}[O_x] &= \frac{d}{dt}([O_3] + [O]) = \frac{d}{dt}[O_3] + \frac{d}{dt}[O] \\ &= [\text{rate}(2) - \text{rate}(3) - \text{rate}(4)] + [2\text{x rate}(1) + \text{rate}(3) - \text{rate}(2) - \text{rate}(4)] \\ &= 2\text{x rate}(1) - 2\text{x rate}(4) \end{aligned} \tag{10.6}$$

Values of τ_{Ox} computed from *(10.5)* range from less than a day in the upper stratosphere to several years in the lower stratosphere, reflecting the abundance of O atoms (Figure 10-4, problem 10. 2). In the upper stratosphere at least, the lifetime of O_x is sufficiently short that chemical steady state can be assumed to hold. This steady state is defined by

$$2k_1[O_2] = 2k_4[O][O_3] \tag{10.7}$$

Substituting *(10.4)* into *(10.7)* yields as solution for $[O_3]$:

$$[O_3] = \left(\frac{k_1k_2}{k_3k_4}\right)^{\frac{1}{2}} C_{O2}n_a^{\frac{3}{2}} \tag{10.8}$$

The simplicity of equation *(10.8)* is deceiving. Calculating $[O_3]$ from this equation is actually not straightforward because the photolysis rate constants $k_1(z)$ and $k_3(z)$ at altitude z depend on the local actinic flux $I_\lambda(z)$, which is attenuated due to absorption of radiation by the O_2 and O_3 columns overhead. From *(9.13)*, the general expression for a photolysis rate constant is

$$k = \int_\lambda q_X(\lambda)\sigma_X(\lambda)I_\lambda d\lambda \tag{10.9}$$

The actinic flux $I_\lambda(z)$ at altitude z is attenuated relative to its value $I_{\lambda,\infty}$ at the top of the atmosphere by

$$I_\lambda(z) = I_{\lambda,\infty}e^{-\frac{\delta}{\cos\theta}} \tag{10.10}$$

where θ is the solar zenith angle, that is the angle between the Sun and the vertical (section 7.6), and δ is the optical depth of the atmosphere above z computed from *(7.30)*:

$$\delta = \int_z^\infty (\sigma_{O2}[O_2] + \sigma_{O3}[O_3])dz' \tag{10.11}$$

Values of I_λ at UV wavelengths decrease rapidly with decreasing altitude in the stratosphere because of efficient absorption by O_2 and O_3 (Figure 10-2), and k_1 and k_3 decrease correspondingly (Figure 10-5).

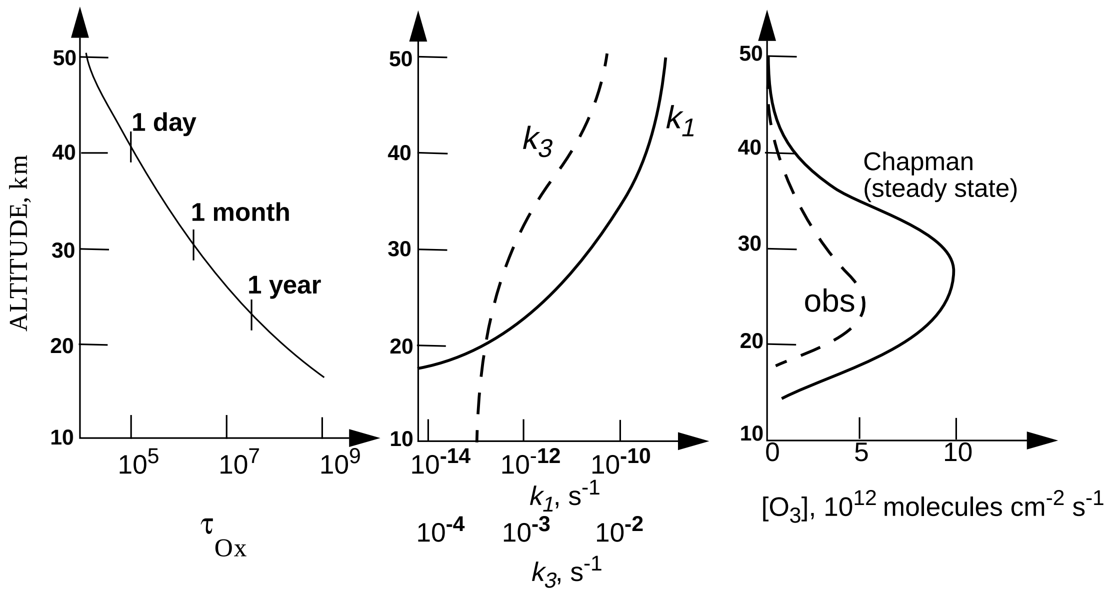

Figure 10-5 Chapman mechanism at low latitudes. Left panel: Lifetime of O_x. Center panel: O_2 and O_3 photolysis rate constants. Right panel: calculated and observed vertical profiles of O_3 concentrations.

Since $k_1(z)$ and $k_3(z)$ depend on the O_3 column overhead through *(10.9)-(10.11)*, equation *(10.8)* is not explicit for [O_3] (the right-hand-side depends on [O_3]). Solution to *(10.8)* must be obtained numerically by starting from the top of the atmosphere with $I_\lambda = I_{\lambda,\infty}$ and [O_3] = 0, and progressing downward by small increments in the atmosphere, calculating $I_\lambda(z)$ and the resulting values of $k_1(z)$, $k_3(z)$, and $[O_3](z)$ as one penetrates in the atmosphere.

The resulting solution (Figure 10-5, right panel) is able to explain at least qualitatively the observed maximum of O_3 concentrations at 20-30 km altitude. The maximum reflects largely the vertical dependence of O_x production by *(R1)*, $2k_1[O_2]$, which we have seen is the effective source for O_3. The O_2 number density decreases exponentially with altitude following the barometric law, while k_1 decreases sharply with decreasing altitude due to absorption of UV radiation by O_3 and O_2. The product $k_1[O_2]$ thus has a maximum value at 20-30 km altitude. See problem 10. 1 for an analytical derivation of this maximum.

Although the Chapman mechanism is successful in reproducing the general shape of the O_3 layer, it overestimates the observed O_3 concentrations by a factor of 2 or more (Figure 10-5). In the lower stratosphere, a steady state solution to the mechanism would not necessarily be expected because of the long lifetime of O_x; there, transport may play a dominant role in shaping the O_3 distribution. In the upper stratosphere, however, where the lifetime of O_x is short, the discrepancy between theory and observations points to a flaw in the theory. Either the source of O_x in the Chapman mechanism is too large, or the sink is too small. Considering that the source from *(R1)* is well constrained by spectroscopic data, the logical conclusion is that there must be additional sinks for O_3 not accounted for by the Chapman mechanism. This flaw was not evident until the 1950s, because the relatively poor quality of the stratospheric ozone observations and the uncertainties on the rate constants of reactions *(R1)-(R4)* could accommodate the discrepancies between theory and observations. As the experimental data base improved, however, the discrepancy became clear.

10.2 CATALYTIC LOSS CYCLES

10.2.1 Hydrogen oxide radicals (HO_x)

In the late 1950s it was discovered that catalytic cycles initiated by oxidation of water vapor could represent a significant sink for O_3 in the stratosphere. Water vapor is supplied to the stratosphere by transport from the troposphere, and is also produced within the stratosphere by oxidation of CH_4. Water vapor mixing ratios in the stratosphere are relatively uniform, in the range 3-5 ppmv. In the stratosphere, water vapor is oxidized by $O(^1D)$ produced from *(R3)*:

$$H_2O + O(^1D) \rightarrow 2OH \qquad \text{(R5)}$$

The high-energy $O(^1D)$ atoms are necessary to overcome the stability of the H_2O molecule.

The hydroxyl radical OH produced by *(R5)* can react with O_3, producing the hydroperoxy radical HO_2 which in turn reacts with

O_3:

$$OH + O_3 \rightarrow HO_2 + O_2 \tag{R6}$$

$$HO_2 + O_3 \rightarrow OH + 2O_2 \tag{R7}$$

$$\text{Net:} \quad 2O_3 \rightarrow 3O_2$$

We refer to the ensemble of OH and HO_2 as the HO_x chemical family. The sequence of reactions *(R6)* and *(R7)* consumes O_3 while conserving HO_x. Therefore HO_x acts as a *catalyst* for O_3 loss; production of one HO_x molecule by *(R5)* can result in the loss of a large number of O_3 molecules by cycling of HO_x through *(R6)* and *(R7)*. Termination of the catalytic cycle requires loss of HO_x by a reaction such as

$$OH + HO_2 \rightarrow H_2O + O_2 \tag{R8}$$

The sequence *(R5)-(R8)* is a *chain reaction* for O_3 loss in which *(R5)* is the *initiation step*, *(R6)-(R7)* are the *propagation steps*, and *(R8)* is the *termination step*. There are several variants to the HO_x-catalyzed mechanism, involving reactions other than *(R6)-(R8)*; see problem 10. 4. From knowledge of stratospheric water vapor concentrations and rate constants for *(R5)-(R8)*, and assuming chemical steady state for the HO_x radicals (a safe assumption in view of their short lifetimes), one can calculate the O_3 loss rate. Such calculations conducted in the 1950s and 1960s found that HO_x catalysis was a significant O_3 sink but not sufficient to reconcile the chemical budget of O_3. Nevertheless, the discovery of HO_x catalysis introduced the important new idea that species present at trace levels in the stratosphere could trigger chain reactions destroying O_3. This concept was to find its crowning application in subsequent work, as described below. Another key advance was the identification of *(R5)* as a source for the OH radical, a strong oxidant. As we will see in chapter 11, oxidation by OH provides the principal sink for a large number of species emitted in the atmosphere. Finally, recent work has shown that the HO_x-catalyzed mechanism represents in fact the dominant sink of O_3 in the lowest part of the stratosphere (section 10.4).

10.2.2 Nitrogen oxide radicals (NO_x)

The next breakthrough in our understanding of stratospheric O_3

came about in the late 1960s when the United States and other countries considered the launch of a supersonic aircraft fleet flying in the stratosphere. Atmospheric chemists were called upon to assess the effects of such a fleet on the O_3 layer. An important component of aircraft exhaust is nitric oxide (NO) formed by oxidation of atmospheric N_2 at the high temperatures of the aircraft engine. In the stratosphere NO reacts rapidly with O_3 to produce NO_2, which then photolyzes:

$$NO + O_3 \rightarrow NO_2 + O_2 \tag{R9}$$

$$NO_2 + h\nu \rightarrow NO + O \tag{R10}$$

$$O + O_2 + M \rightarrow O_3 + M \tag{R2}$$

This cycling between NO and NO_2 takes place on a time scale of about one minute during daytime. It has no net effect on O_3 and is called a *null cycle*. It causes, however, rapid exchange between NO and NO_2. We refer to the ensemble of NO and NO_2 as a new chemical family, NO_x.

Further investigation of NO_x chemistry in the stratosphere showed that a fraction of the NO_2 molecules produced by *(R9)* reacts with oxygen atoms produced by *(R3)*:

$$NO_2 + O \rightarrow NO + O_2 \tag{R11}$$

The sequence of reactions *(R9)* and *(R11)* represents a catalytic cycle for O_3 loss with a net effect identical to *(R4)*:

$$NO + O_3 \rightarrow NO_2 + O_2 \tag{R9}$$

$$NO_2 + O \rightarrow NO + O_2 \tag{R11}$$

$$\text{net:} \quad O_3 + O \rightarrow 2O_2$$

Each cycle consumes two O_x molecules, which is equivalent to two O_3 molecules (see section 10.1.2). The rate-limiting step in the cycle is *(R11)* because NO_2 has the option of either photolyzing (null cycle) or reacting with O (O_3 loss cycle). The O_3 loss rate is therefore given by

$$-\frac{d}{dt}[O_3] \approx -\frac{d}{dt}[O_x] = 2k_{11}[NO_2][O] \tag{10.12}$$

Termination of the catalytic cycle involves loss of NO_x radicals. In the daytime, NO_x is oxidized to HNO_3 by the strong radical oxidant OH (section 10.2.1):

$$NO_2 + OH + M \rightarrow HNO_3 + M \tag{R12}$$

At night OH is absent, because there is no $O(^1D)$ to oxidize H_2O by *(R5)*. Loss of NO_x at night takes place through the oxidation of NO_2 by O_3 and subsequent conversion of the NO_3 radical to N_2O_5:

$$NO_2 + O_3 \rightarrow NO_3 + O_2 \tag{R13}$$

$$NO_3 + NO_2 + M \rightarrow N_2O_5 + M \tag{R14}$$

This formation of N_2O_5 can take place only at night, because during daytime NO_3 is photolyzed back to NO_2 on a time scale of a few seconds:

$$NO_3 + h\nu \rightarrow NO_2 + O \tag{R15}$$

The products of NO_x oxidation, HNO_3 and N_2O_5, are non-radical species and have therefore relatively long lifetimes against chemical loss (weeks for HNO_3, hours to days for N_2O_5). They are eventually converted back to NO_x:

$$HNO_3 + h\nu \rightarrow NO_2 + OH \tag{R16}$$

$$HNO_3 + OH \rightarrow NO_3 + H_2O \tag{R17}$$

$$NO_3 + h\nu \rightarrow NO_2 + O \tag{R15}$$

$$N_2O_5 + h\nu \rightarrow NO_3 + NO_2 \tag{R18}$$

and serve therefore as *reservoirs* for NO_x. We refer to the ensemble of NO_x and its reservoirs as yet another chemical family, NO_y. Ultimate removal of NO_y is by transport to the troposphere where HNO_3 is rapidly removed by deposition.

A diagram of the ensemble of processes is shown in Figure 10-6. The loss rate of O_3 can be calculated from knowledge of the aircraft emission rate of NO, the chemical cycling within the NO_y family, and the residence time of air (and therefore NO_y) in the stratosphere. Model calculations conducted in the 1970s found that an aircraft fleet in the stratosphere would represent a serious threat to the O_3 layer. This environmental concern, combined with economic considerations, led to scrapping of the supersonic aircraft plan in the United States (the Europeans still built the Concorde).

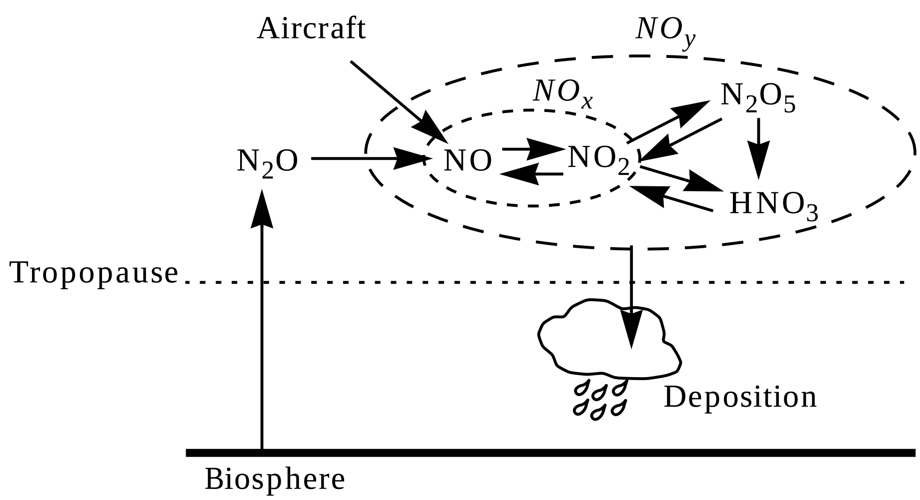

Figure 10-6 Sources and sinks of stratospheric NO_x and NO_y. The direct conversion of N_2O_5 to HNO_3 takes place in aerosols and will be discussed in section 10.4.

The identification of a NO_x-catalyzed mechanism for O_3 loss turned out to be a critical lead towards identifying the missing O_3 sink in the Chapman mechanism. Beyond the source from supersonic aircraft, could there be a *natural* source of NO_x to the stratosphere? Further work in the early 1970s showed that N_2O, a low-yield product of nitrification and denitrification processes in the biosphere (section 6.3), provides such a source. N_2O is a very stable molecule which has no significant sinks in the troposphere. It is therefore transported to the stratosphere where it encounters high concentrations of $O(^1D)$, allowing oxidation to NO by

$$N_2O + O(^1D) \rightarrow 2NO \qquad \text{(R19)}$$

Reaction *(R19)* actually accounts for only about 5% of loss of N_2O in the stratosphere; the remaining 95% are converted to N_2 by photolysis and oxidation by $O(^1D)$ via an alternate branch. The conversion to N_2 is however of no interest for driving stratospheric chemistry.

On the basis of Figure 10-6, we see that the loss rate of O_3 by the NO_x-catalyzed mechanism can be calculated from knowledge of the production and loss rates of NO_y, and of the chemical cycling within the NO_y family. We examine now our ability to quantify each of these terms:

- *Production rate of NO_y.* In the natural stratosphere, NO_y is produced as NO from oxidation of N_2O by $O(^1D)$. The concentration of N_2O in the stratosphere is readily measurable by spectroscopic methods, and the concentration of $O(^1D)$ can be calculated from chemical steady state by reaction *(R3)*, so that the source of NO_y is well constrained.
- *Loss rate of NO_y.* The dominant sink for NO_y in the stratosphere is transport to the troposphere followed by deposition. We saw in chapter 4 that the residence time of air (and hence of NO_y) in the stratosphere is 1-2 years. Thus the loss rate of NO_y is relatively well constrained, to within a factor of two.
- *Chemical cycling within the NO_y family.* The rate of O_3 loss depends on the fraction of NO_y present as NO_x, that is, the NO_x/NO_y ratio. This ratio can be calculated from the rate equations for the different components of the NO_y family. Under most conditions, chemical steady state between the different NO_y components is a good approximation.

We therefore have all the elements needed to calculate the O_3 loss rate from the NO_x-catalyzed mechanism. When atmospheric chemists did these calculations in the 1970s they found that they could fully account for the missing sink of O_3 in the Chapman mechanism! Figure 10-7 shows results from such a calculation constrained with simultaneous observations of NO_y, O_3, H_2O, and CH_4 through the depth of the stratosphere. The O_x loss rates in this calculation are computed on the basis of the gas-phase mechanisms described above, and the resulting total O_x loss (solid line) is compared to the source of O_x from photolysis of O_2 (long dashes). Results show a close balance between O_x production and loss, with NO_x catalysis providing the dominant sink in most of the stratosphere. The budget of stratospheric O_3 finally appeared to be closed. Paul Crutzen received the 1995 Nobel Prize in Chemistry for this work.

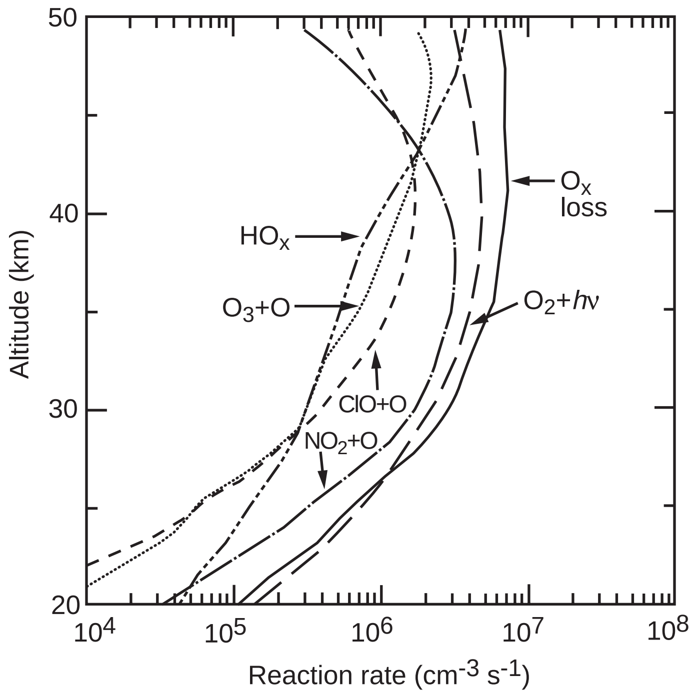

Figure 10-7 24-hour average rates of O_x production and loss computed with a gas-phase chemistry model constrained with simultaneous observations of O_3, H_2O, CH_4, NO_y, and Cl_y from the space shuttle. We will see in section 10.4 that consideration of aerosol chemistry modifies greatly the model results in the lower stratosphere. From McElroy, M.B., and R.J. Salawitch, *Science 243,* 763-770, 1989.

Ice core data show that atmospheric concentrations of N_2O have risen from 285 ppbv in the 18th century to 310 ppbv today, and present-day atmospheric observations indicate a growth rate of 0.3 % yr^{-1} (Figure 7-1). There is much interest in understanding this rise because of the importance of N_2O not only as a sink for stratospheric O_3 but also as a greenhouse gas (chapter 7). Table 10.1 gives current estimates of the sources and sinks of atmospheric N_2O. Although the estimates can provide a balanced budget within their ranges of uncertainty (atmospheric increase ≈ sources - sinks), the uncertainties are in fact large. Biogenic sources in the tropical continents, cultivated areas, and the oceans provide the dominant sources of N_2O. The increase of N_2O over the past century is thought to be due principally to increasing use of fertilizer for agriculture.

Table 10-1 Present-day global budget of N_2O

	Rate, Tg N yr^{-1} best estimate and range of uncertainty
SOURCES, natural	**9 (6-12)**
Oceans	3 (1-5)
Tropical soils	4 (3-6)
Temperate soils	2 (0.6-4)
SOURCES, anthropogenic	**6 (4-8)**
Cultivated soils	4 (2-5)
Biomass burning	0.5 (0.2-1.0)
Chemical industry	1.3 (0.7-1.8)
Livestock	0.4 (0.2-0.5)
SINK Stratosphere	**12 (9-16)**
ATMOSPHERIC INCREASE	**4**

10.2.3 Chlorine radicals (ClO_x)

In 1974, Mario Molina and Sherwood Rowland pointed out the potential for O_3 loss associated with rising atmospheric concentrations of chlorofluorocarbons (CFCs). CFCs are not found in nature; they were first manufactured for industrial purposes in the 1930s and their use increased rapidly in the following decades. During the 1970s and 1980s, atmospheric concentrations of CFCs rose by 2-4% yr^{-1} (Figure 7-1). CFC molecules are inert in the troposphere; they are therefore transported to the stratosphere, where they photolyze to release Cl atoms. For example, in the case of CF_2Cl_2 (known by the trade name CFC-12):

$$CF_2Cl_2 + h\nu \rightarrow CF_2Cl + Cl \qquad \text{(R20)}$$

The Cl atoms then trigger a catalytic loss mechanism for O_3 involving cycling between Cl and ClO (the ClO_x family). The sequence is similar to that of the NO_x-catalyzed mechanism:

$$Cl + O_3 \rightarrow ClO + O_2 \tag{R21}$$

$$ClO + O \rightarrow Cl + O_2 \tag{R22}$$

$$\text{net:} \qquad O_3 + O \rightarrow 2O_2$$

The rate-limiting step for O_3 loss in this cycle is *(R22)* (see problem 10. 5), so that the O_3 loss rate is

$$-\frac{d}{dt}[O_3] = -\frac{d}{dt}[O_x] = 2k_{22}[ClO][O] \tag{10.13}$$

The catalytic cycle is terminated by conversion of ClO_x to non-radical chlorine reservoirs, HCl and $ClNO_3$:

$$Cl + CH_4 \rightarrow HCl + CH_3 \tag{R23}$$

$$ClO + NO_2 + M \rightarrow ClNO_3 + M \tag{R24}$$

The lifetime of HCl is typically a few weeks and the lifetime of $ClNO_3$ is of the order of a day. Eventually these reservoirs return ClO_x:

$$HCl + OH \rightarrow Cl + H_2O \tag{R25}$$

$$ClNO_3 + h\nu \rightarrow Cl + NO_3 \tag{R26}$$

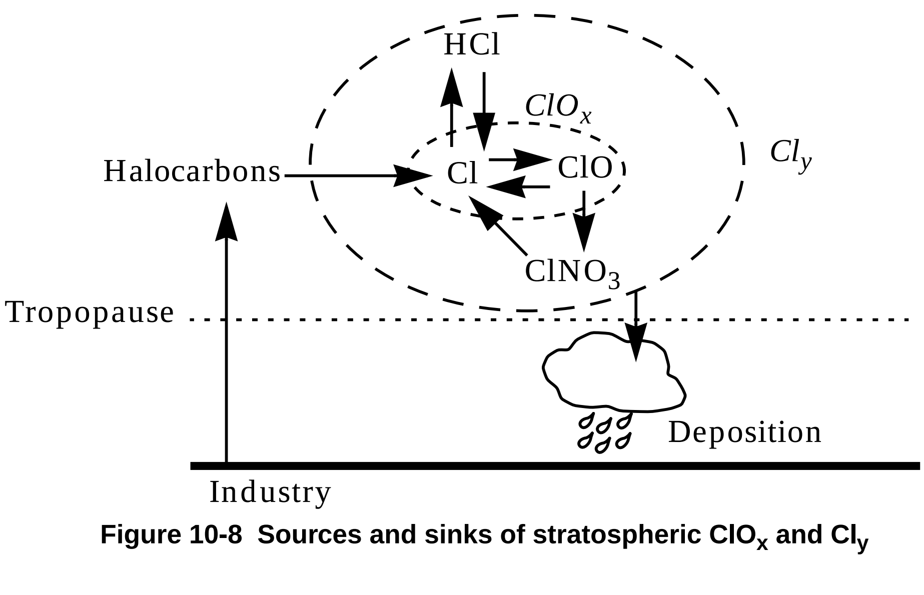

Figure 10-8 Sources and sinks of stratospheric ClO_x and Cl_y

We thus define a chemical family Cl_y as the sum of ClO_x and its reservoirs. A diagram of the ensemble of processes is shown in Figure 10-8. Note the similarity to Figure 10-6.

Similarly to the NO_x-catalyzed mechanism, the rate of O_3 loss by the ClO_x-catalyzed mechanism can be calculated from knowledge of the concentrations of CFCs and other halocarbons in the stratosphere, the residence time of air in the stratosphere, and the ClO_x/Cl_y chemical partitioning. Molina and Rowland warned that ClO_x-catalyzed O_3 loss would become a significant threat to the O_3 layer as CFC concentrations continued to increase. Their warning, backed up over the next two decades by increasing experimental evidence and compounded by the discovery of the antarctic ozone hole, led to a series of international agreements (beginning with the Montreal protocol in 1987) which eventually resulted in a total ban on CFC production as of 1996. For this work they shared the 1995 Nobel Prize in Chemistry with Paul Crutzen.

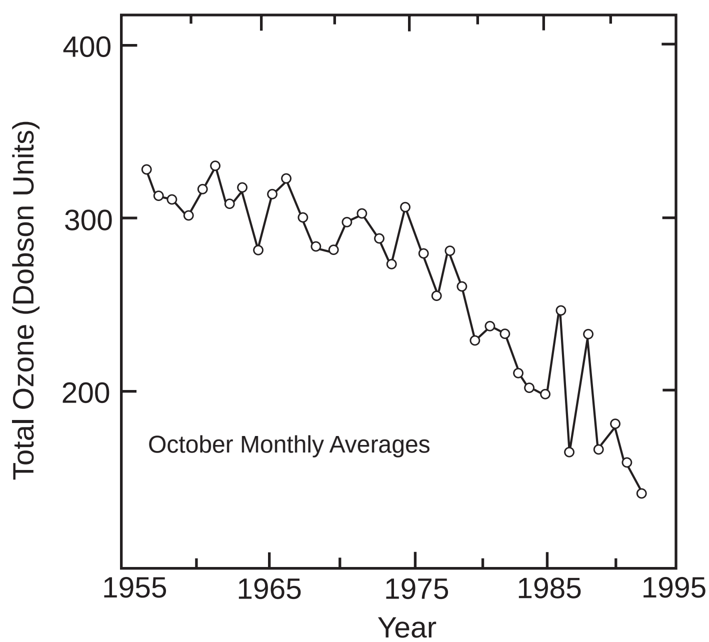

Figure 10-9 Historical trend in the total ozone column measured spectroscopically over Halley Bay, Antarctica in October, 1957-1992. One Dobson unit (DU) represents a 0.01 mm thick layer of ozone under standard conditions of temperature and pressure; 1 DU = 2.69×10^{16} molecules $cm^{-2}s^{-1}$. From: *Scientific Assessment of Ozone Depletion: 1994,* World Meteorological Organization (WMO), Geneva,1995.

10.3 POLAR OZONE LOSS

In 1985, a team of scientists from the British Antarctic Survey reported that springtime stratospheric O_3 columns over their station at Halley Bay had decreased precipitously since the 1970s (Figure 10-9). The depletion was confined to the spring months (September-November); no depletion was observed in other seasons. Global satellite data soon confirmed the Halley Bay observations and showed that the depletion of stratospheric O_3 extended over the totality of the *antarctic vortex*, a large circumpolar region including most of the southern polar latitudes. The depletion of O_3 has worsened since 1985, and springtime O_3 columns over Antarctica today are less than half of what they were in the 1960s (Figure 10-9). Measured vertical profiles show that the depletion of O_3 is essentially total in the lowest region of the stratosphere between 10 and 20 km (Figure 10-10), which normally would contain most of the total O_3 column in polar spring (Figure 10-1).

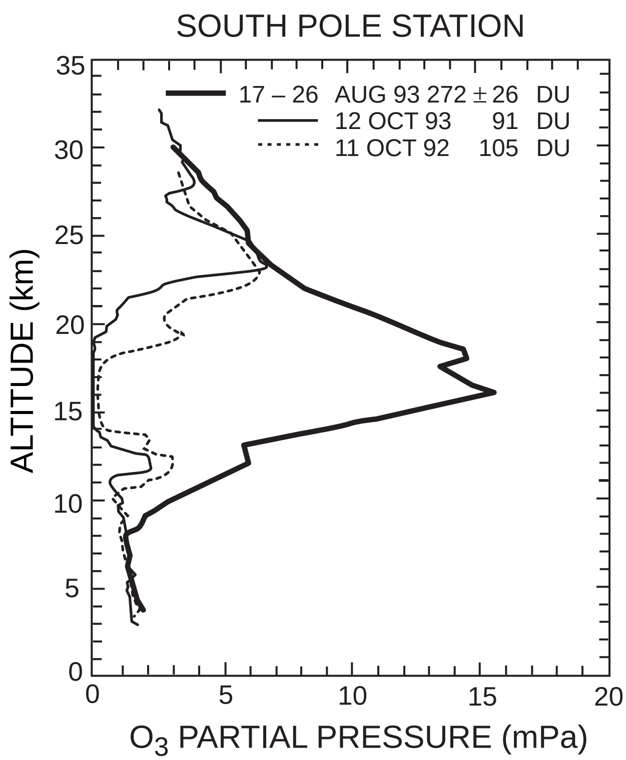

Figure 10-10 Vertical profiles of ozone over Antarctica measured by chemical sondes. In August the ozone hole has not developed yet, while in October it is fully developed. From Harris, N.R.P., et al., Ozone measurements, in WMO, op. cit..

Discovery of this “antarctic ozone hole” (as it was named in the popular press) was a shock to atmospheric chemists, who thought by then that the factors controlling stratospheric O_3 were relatively well understood. The established mechanisms presented in sections 10.1 and 10.2 could not explain the O_3 depletion observed over Antarctica. Under the low light conditions in that region, concentrations of O atoms are very low, so that reactions *(R11)* and *(R22)* cannot operate at a significant rate. This severe failure of theory sent atmospheric chemists scrambling to understand what processes were missing from their understanding of stratospheric chemistry, and whether the appearance of the antarctic O_3 hole could be a bellwether of future catastrophic changes in stratospheric O_3 levels over other regions of the world.

10.3.1 Mechanism for ozone loss

Several aircraft missions were conducted in the late 1980s to understand the causes of the antarctic ozone depletion. These studies found the depletion of O_3 to be associated with exceptionally high ClO, a result confirmed by satellite data. Parallel laboratory experiments showed that at such high ClO concentrations, a new catalytic cycle involving self-reaction of ClO could account for most of the observed O_3 depletion:

$$ClO + ClO + M \rightarrow ClOOCl + M \qquad \text{(R27)}$$

$$ClOOCl + h\nu \rightarrow ClOO + Cl \qquad \text{(R28)}$$

$$ClOO + M \rightarrow Cl + O_2 \qquad \text{(R29)}$$

$$\text{(2x)} \quad Cl + O_3 \rightarrow ClO + O_2 \qquad \text{(R21)}$$

$$\text{net:} \quad 2O_3 \rightarrow 3O_2$$

The key behind discovery of this catalytic cycle was the laboratory observation that photolysis of the ClO dimer (ClOOCl) takes place at the O-Cl bond rather than at the weaker O-O bond. It was previously expected that photolysis would take place at the O-O bond, regenerating ClO and leading to a null cycle. The rate of O_3 loss in the catalytic cycle is found to be limited by *(R27)* and is therefore quadratic in [ClO]; it does not depend on the abundance of O atoms, in contrast to the ClO_x-catalyzed mechanism described in the previous section.

Another catalytic cycle found to be important in the depletion of O_3 during antarctic spring involves Br radicals produced in the stratosphere by photolysis and oxidation of anthropogenic Br-containing gases such as CH_3Br (see problem 6. 4):

$$Cl + O_3 \rightarrow ClO + O_2 \qquad \text{(R21)}$$

$$Br + O_3 \rightarrow BrO + O_2 \qquad \text{(R30)}$$

$$BrO + ClO \rightarrow Br + Cl + O_2 \qquad \text{(R31)}$$

Again, this catalytic cycle is made significant by the high concentrations of ClO over Antarctica. According to current models, the ClO+ClO mechanism accounts for about 70% of total O_3 loss in the antarctic ozone hole; the remaining 30% is accounted for by the BrO+ClO mechanism.

Why are ClO concentrations over Antarctica so high? Further research in the 1990s demonstrated the critical role of reactions taking place in stratospheric aerosols at low temperature. Temperatures in the wintertime antarctic stratosphere are sufficiently cold to cause formation of persistent ice-like clouds called polar stratospheric clouds (PSCs) in the lower part of the stratosphere. The PSC particles provide surfaces for conversion of the ClO_x reservoirs HCl and $ClNO_3$ to Cl_2, which then rapidly photolyzes to produce ClO_x:

$$ClNO_3 + HCl \xrightarrow{PSC} Cl_2 + HNO_3 \qquad \text{(R32)}$$

$$Cl_2 + h\nu \rightarrow 2Cl \qquad \text{(R33)}$$

Reaction *(R32)* is so fast that it can be regarded as quantitative; either $ClNO_3$ or HCl is completely titrated. Whereas in most of the stratosphere the ClO_x/Cl_y molar ratio is less than 0.1, in the antarctic vortex it exceeds 0.5 and can approach unity. Recent research indicates that *(R32)* proceeds rapidly not only on PSC surfaces but also in the aqueous H_2SO_4 aerosols present ubiquitously in the stratosphere (section 8.1) when the temperatures fall to the values observed in antarctic winter (below 200 K). Low temperature rather than the presence of PSCs appears to be the critical factor for *(R32)* to take place. Nevertheless, as we will see below, PSCs play a critical role in the development of the O_3 hole by providing a mechanism for removal of HNO_3 from the stratosphere.

10.3.2 PSC formation

Because the stratosphere is extremely dry, condensation of water vapor to form ice clouds requires extremely low temperatures. The stratospheric mixing ratio of water vapor is relatively uniform at

3-5 ppmv. In the lower stratosphere at 100 hPa (16 km altitude), this mixing ratio corresponds to a water vapor pressure of 3-5x10^{-4} hPa. The frost point at that vapor pressure is 185-190 K; such low temperatures are almost never reached except in antarctic winter. When temperatures do fall below 190 K, PSCs are systematically observed. Observations show however that PSCs start to form at a higher temperature, about 197 K (Figure 10-11), and this higher temperature threshold for PSC formation is responsible for the large extent of the O_3 hole.

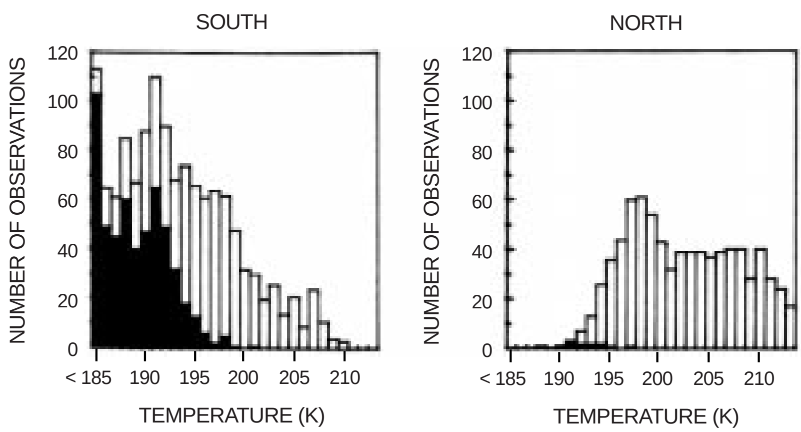

Figure 10-11 Frequency distributions of temperature (total bars) and PSC occurrence (shaded bars) in the winter lower stratosphere of each hemisphere at 65°-80° latitude. Adapted from McCormick, M.P., et al., *J. Atmos. Sci., 39,* 1387, 1982.

Discovery of the antarctic ozone hole spurred intense research into the thermodynamics of PSC formation. It was soon established that the stratosphere contains sufficiently high concentrations of HNO_3 that solid HNO_3-H_2O phases may form at temperatures higher than the frost point of water. These solid phases are:

- $HNO_3 \cdot 3H_2O$ - Nitric acid trihydrate (NAT)
- $HNO_3 \cdot 2H_2O$ - Nitric acid dihydrate (NAD)
- $HNO_3 \cdot H_2O$ - Nitric acid monohydrate (NAM)

Figure 10-12 is a phase diagram for the binary HNO_3-H_2O system. The diagram shows the thermodynamically stable phases of the system as a function of P_{HNO3} and P_{H2O}. There are six different phases in the diagram: NAT, NAD, NAM, H_2O ice, liquid HNO_3-H_2O solution, and gas. The presence of a gas phase is implicit in the choice of P_{HNO3} and P_{H2O} as coordinates. From the phase rule, the number n of independent variables defining the thermodynamically stable phases(s) of the system is

$$n = c + 2 - p \tag{10.14}$$

where c is the number of components of the system (here two: HNO_3 and H_2O), and p is the number of phases present at equilibrium. Equilibrium of a PSC phase with the gas phase ($p = 2$) is defined by two independent variables (n = 2). If we are given the HNO_3 and H_2O vapor pressures (representing *two* independent variables), then we can define unambiguously the composition of the thermodynamically stable PSC and the temperature at which it forms. That is the information given in Figure 10-12.

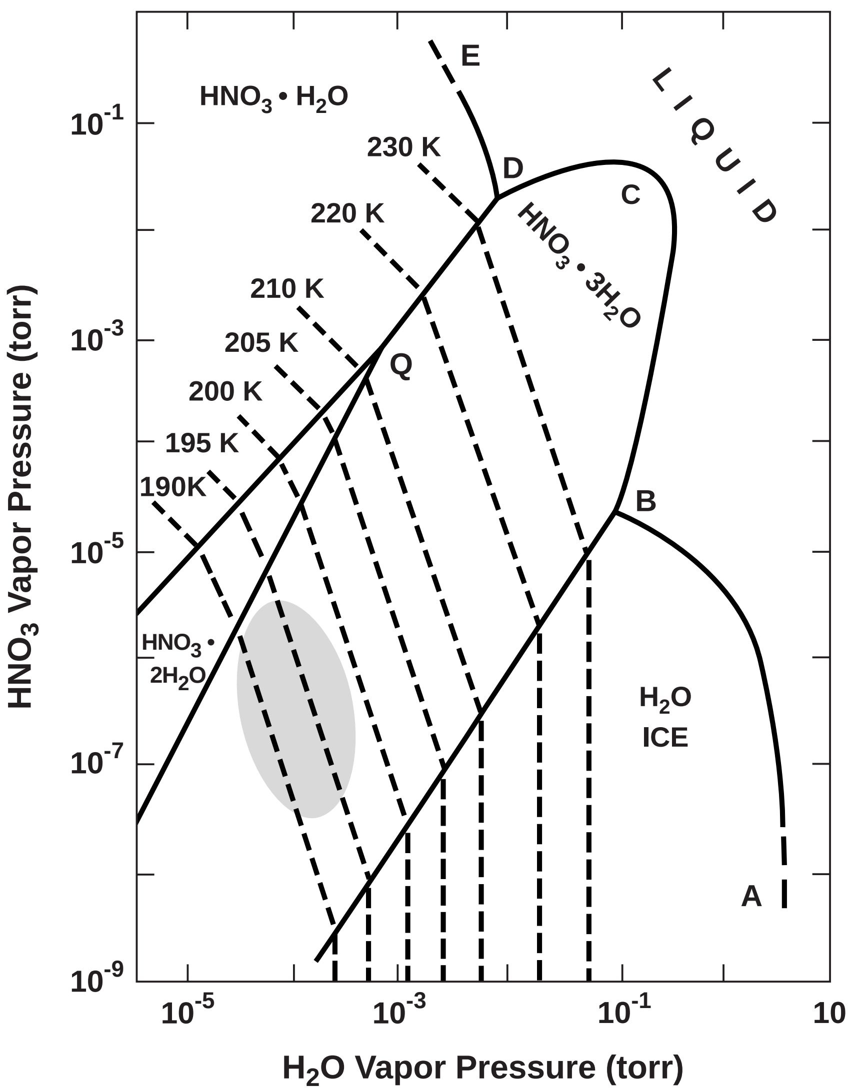

Figure 10-12 Phase diagram for the HNO_3-H_2O system. The shaded area identifies typical ranges of P_{HNO3} and P_{H2O} in the lower stratosphere.

The shaded region in Figure 10-12 indicates the typical ranges of P_{HNO3} and P_{H2O} in the lower stratosphere. We see that condensation of NAT is possible at temperatures as high as 197 K, consistent with the PSC observations. It appears from Figure 10-12 that NAT represents the principal form of PSCs; pure water ice PSCs can also form under particularly cold conditions (problem 10. 10). Recent investigations show that additional PSC phases form in the ternary HNO_3-H_2SO_4-H_2O system.

10.3.3 Chronology of the ozone hole

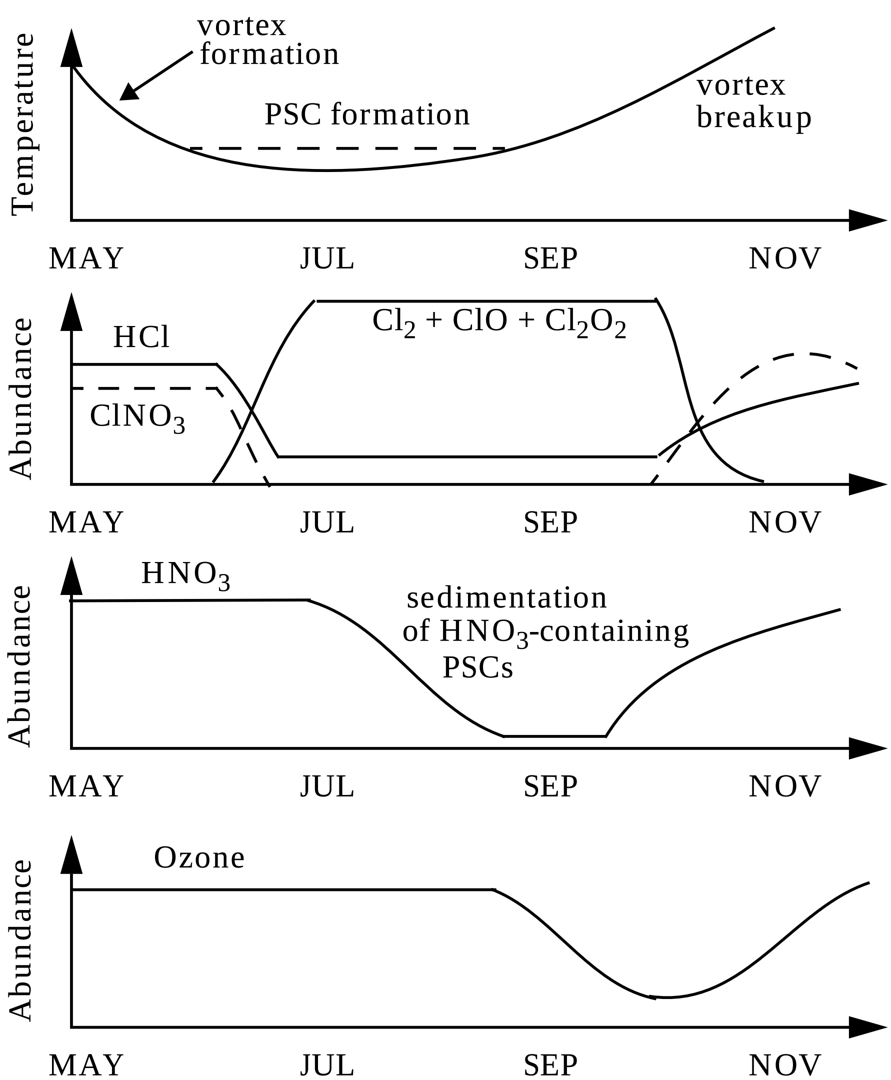

Figure 10-13 Chronology of the antarctic ozone hole

The chronology of the antarctic ozone hole is illustrated in Figure 10-13. It begins with the formation of the antarctic vortex in austral fall (May). As we saw in chapter 4, there is a strong westerly circulation at southern midlatitudes resulting from the contrast in heating between the tropics and polar regions. Because of the lack of topography or land-ocean contrast to disturb the westerly flow at southern midlatitudes, little meridional transport takes place and the antarctic atmosphere is effectively isolated from lower latitudes. This isolation is most pronounced during winter, when the latitudinal heating gradient is strongest. The isolated antarctic air mass in winter is called the *antarctic vortex* because of the strong circumpolar circulation.

By June, temperatures in the antarctic vortex have dropped to values sufficiently low for PSC formation. Reaction *(R32)* then converts HCl and $ClNO_3$ to Cl_2, which photolyzes to yield Cl atoms. In the winter, however, loss of O_3 is limited by the lack of solar radiation to photolyze the ClOOCl dimer produced in *(R27)*. Significant depletion of O_3 begins only in September when sufficient light is available for ClOOCl photolysis to take place rapidly.

By September, however, temperatures have risen sufficiently that all PSCs have evaporated. One would then expect HNO_3 in the vortex to scavenge ClO_x by

$$HNO_3 + h\nu \rightarrow NO_2 + OH \qquad \text{(R16)}$$

followed by

$$ClO + NO_2 + M \rightarrow ClNO_3 + M \qquad \text{(R24)}$$

suppressing O_3 loss. This removal of ClO_x is found to be inefficient, however, because observed HNO_3 concentrations in the springtime antarctic vortex are exceedingly low (Figure 10-13). Depletion of HNO_3 from the antarctic stratosphere is caused by sedimentation of HNO_3-containing PSC particles over the course of the winter; it is still not understood how the PSC particles grow to sufficiently large sizes to undergo sedimentation. Better understanding of this sedimentation process is critical for assessing the temporal extent of the antarctic ozone hole, and also for predicting the possibility of similar O_3 depletion taking place in the arctic.

There is indeed much concern at present over the possibility of an O_3 hole developing in the arctic. Temperatures in arctic winter occasionally fall to values sufficiently low for PSCs to form and for HCl and $ClNO_3$ to be converted to ClO_x (Figure 10-11), but these conditions are generally not persistent enough to allow removal of HNO_3 by PSC sedimentation. As a result, O_3 depletion in arctic spring is suppressed by *(R16)+(R24)*. If extensive PSC sedimentation were to take place in arctic winter, one would expect the subsequent development of a springtime arctic O_3 hole. Observations indicate that the arctic stratosphere has cooled in recent years, and a strong correlation is found between this cooling and increased O_3 depletion. One proposed explanation for the cooling is increase in the concentrations of greenhouse gases. Greenhouse gases in the stratosphere have a net cooling effect (in contrast to the troposphere) because they radiate away the heat generated from the absorption of UV by O_3. Continued cooling of the arctic stratosphere over the next decades could possibly cause the development of an “arctic ozone hole” even as chlorine levels decrease due to the ban on CFCs. This situation is being closely watched by atmospheric chemists.

10.4 AEROSOL CHEMISTRY

Another major challenge to our understanding of stratospheric chemistry emerged in the early 1990s when long-term observations of O_3 columns from satellites and ground stations revealed large declines in O_3 extending outside the polar regions. The observations (Figure 10-14) indicate a ~6% decrease from 1979 to 1995 in the global mean stratospheric O_3 column at 60^oS-60^oN, with most of the decrease taking place at midlatitudes.

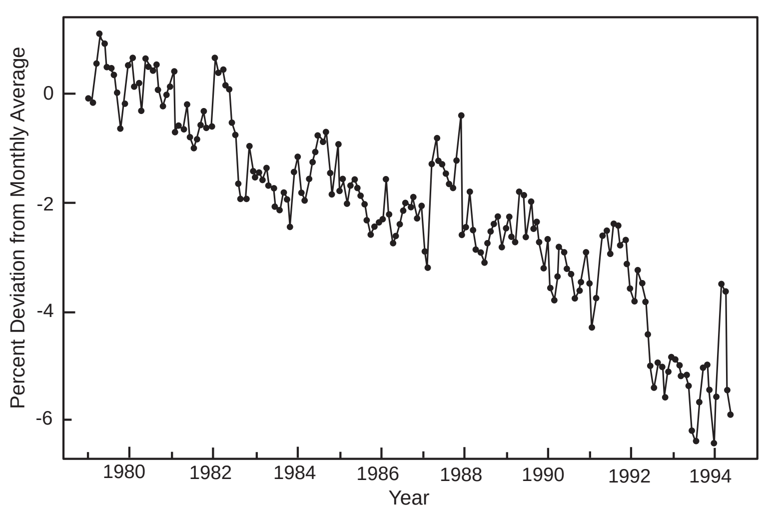

Figure 10-14 Trend in the global ozone column at 60^oS-60^oN for the 1979-1995 period. From WMO, op. cit.

This large decline of O_3 was again a surprise. It was not forecast by the standard gas-phase chemistry models based on the mechanisms in section 10.2, which predicted only a ~0.1% yr^{-1} decrease in the O_3 column for the 1979-1995 period. The models also predicted that most of the O_3 loss would take place in the upper part of the stratosphere, where CFCs photolyze, but observations show that most of the decrease in the O_3 column actually has taken place in the lowermost stratosphere below 20-km altitude (Figure 10-15). This severe failure of the models cannot be explained by the polar chemistry discussed in section 10.3 because temperatures at midlatitudes are too high. Dilution of the antarctic ozone hole when the polar vortex breaks up in summer is not a viable explanation either because it would induce a seasonality and hemispheric asymmetry in the trend that is not seen in the observations.

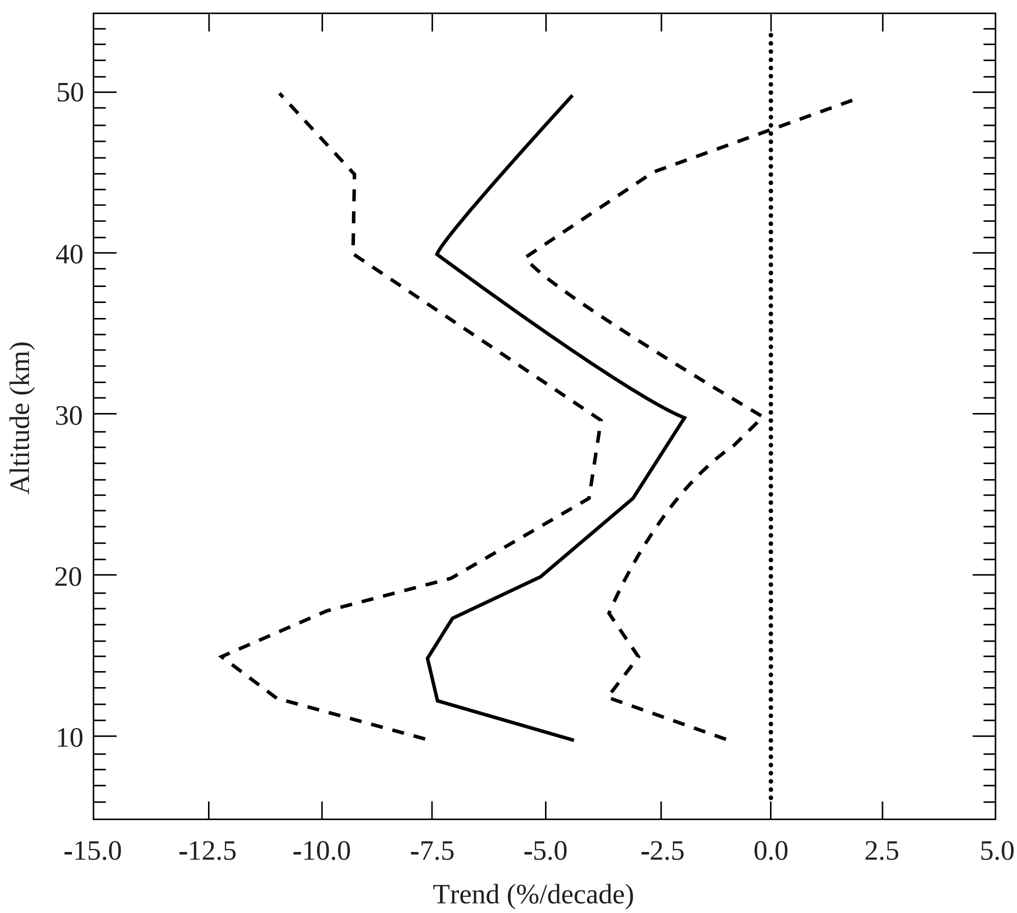

Figure 10-15 Vertical distribution of the O_3 trend at northern midlatitudes for the period 1980-1996: best estimate (solid line) and uncertainties (dashed lines). Adapted from *Scientific Assessment of Ozone Depletion: 1998,* WMO. Geneva ,1999.

Recent research indicates that aerosol chemistry in the lower stratosphere could provide at least a partial explanation for the observed long-term trends of O_3 at midlatitudes. Laboratory experiments have shown that the aqueous H_2SO_4 aerosol ubiquitously present in the lower stratosphere (section 8.1) provides a medium for the rapid hydrolysis of N_2O_5 to HNO_3:

$$N_2O_5 + H_2O \overset{aerosol}{\rightarrow} 2HNO_3 \tag{R34}$$

From the standpoint of the NO_x-catalyzed O_3 loss mechanism discussed in section 10.2.2, *(R34)* simply converts NO_y from one inactive reservoir form to the other. However, HNO_3 is a longer-lived reservoir than N_2O_5, so that conversion of N_2O_5 to HNO_3 slows down the regeneration of NO_x and hence decreases the NO_x/NO_y ratio. Although one might expect O_3 loss to be suppressed as a result, the actual picture is more complicated. Lower NO_x concentrations slow down the deactivation of ClO_x by conversion to $ClNO_3$ *(R24)*, so that ClO_x-catalyzed O_3 loss increases. Also, a fraction of HNO_3 produced by *(R34)* eventually photolyzes by *(R16)*, and the sequence *(R34)+(R16)* provides a source of HO_x that enhances the HO_x-catalyzed O_3 loss discussed in section 10.2.1.

When all these processes are considered, one finds in model calculations that *(R34)* has little net effect on the overall rate of O_3 loss in the lower stratosphere, because the slow-down of the NO_x-catalyzed loss is balanced by the speed-up of the HO_x- and ClO_x-catalyzed losses; in this manner, the gas-phase models of the 1980s were lulled into a false sense of comfort by their ability to balance O_x production and loss (Figure 10-7). The occurrence of *(R34)* implies a much larger sensitivity of O_3 to chlorine levels, which have increased rapidly over the past two decades. Figure 10-16 illustrates this point with model calculations of the relative contributions of different catalytic cycles for O_3 loss, considering gas-phase reactions only (left panel) and including *(R34)* (right panel). Whether or not the enhanced sensitivity to chlorine arising from *(R34)* can explain the observed long-term trends of O_3 (Figure 10-14) is still unclear.

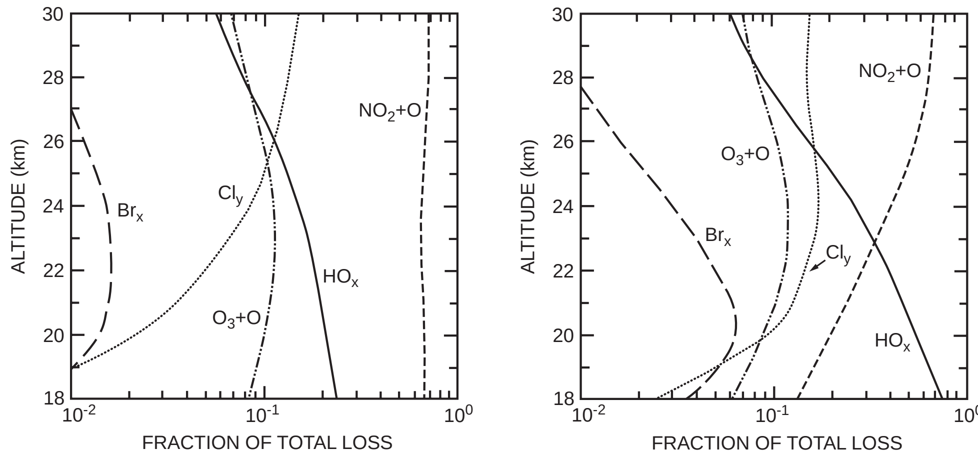

Figure 10-16 Effect of N_2O_5 hydrolysis in aerosols on model calculations of ozone loss in the lower stratosphere at midlatitudes. The Figure shows the fractional contributions of individual processes to the total loss of O_3 in model calculations conducted without (left panel) and with (right panel) hydrolysis of N_2O_5 in aerosols. From McElroy, M.B., et al., The changing stratosphere, *Planet. Space Sci., 40,* 373-401, 1992.

Field observations over the past five years have provided ample evidence that N_2O_5 hydrolysis in aerosols does indeed take place rapidly in the stratosphere. The observed NO_x/NO_y ratio in the lower stratosphere at midlatitudes is lower than expected from purely gas-phase chemistry mechanisms, and more consistent with a mechanism including *(R34).* In addition, the observed ClO/Cl_y ratio is higher than expected from the gas-phase models, because of the slower $ClNO_3$ formation resulting from the lower NO_x levels. Aircraft observations following the Mt. Pinatubo eruption in 1991 indicated large decreases of the NO_x/NO_y ratio and increases of the ClO/Cl_y ratio, as would be expected from *(R34)* taking place on the volcanic aerosols. The resulting enhancement of ClO is thought to be responsible in part for the large decrease in the O_3 column in 1992, the year following the eruption (Figure 10-14).

Further reading:

McElroy, M.B., R.J. Salawitch, and K.R. Minschwaner, The changing stratosphere, *Planet. Space Sci., 40,* **373-401, 1992.** Catalytic loss cycles.

Warneck, P., *Chemistry of the Natural Atmosphere,* **Academic Press, New York, 1988.** Historical survey, photochemistry of O_2 and O_3.

World Meteorological Organization, *Scientific assessment of ozone depletion: 1998,* **WMO, Geneva, 1999.** Polar ozone loss, ozone trends.